JOURNAL OF MATERIALS SCIENCE 21 (1986) 1171–1179

The interaction of molten copper with solid iron

T. ISHIDA
Department of Metallurgical Chemistry, The Research Institute for Iron, Steel and Other Metals, Tohoku University, Sendai 980, Japan

The interaction phenomenon of solid iron with molten copper was studied by investigating the interfacial microstructures of Cu/Fe and Cu–Ag/Fe and the migration mechanism of molten copper and Cu–Ag alloy into the solid iron. A small quantity of copper or Cu–Ag alloy was melted in a solid iron cylindrical specimen at temperatures ranging from 1100 to 1400° C using a high-frequency induction furnace. The Cu/Fe interfacial microstructure consisted of iron dendrites in the copper matrix, and an iron dendrite layer and a copper-penetrated solid solution zone adjacent to each other at the interface. Irrigation effects and grain-boundary penetration were observed partially at lower temperature. The addition of silver to molten copper causes inactivation of the reaction, resulting in the formation of thin reaction layers at the interface. The migration of molten copper and Cu–Ag alloy into solid iron occurs mainly with the formation of an iron-saturated layer due to iron dissolution and a copper-penetrated solid solution zone due to incipient volume diffusion. The copper penetration appears to be dominated by volume diffusion at high temperatures and by both volume and grain-boundary diffusion at low temperatures. Increased silver content in the molten copper decreases the penetration rate constant.

1. Introduction

Interaction of a liquid metal with a solid metal may be composed of the migration of liquid metal into the solid metal and the dissolution of solid metal into the liquid metal. This interaction has given rise to considerable concern in dissimilar metal welding [1], liquid metal corrosion [2], hot galvanizing [3], brazing [4], and the melting of metals in metal containers, etc. In this study, the microstructure and the reaction between molten copper and solid iron were evaluated. The migration of the molten copper into the solid iron was then investigated in connection with the interaction. The principal mechanism of migration of molten copper into solid iron is shown to be by grain-boundary penetration [5, 6]. The reason why this grain-boundary penetration occurs may be due to the lowering of the molten metal/solid metal interfacial energy, which is considerably affected by the alloying element in the base metal iron. However, grain-boundary penetration is not likely to occur with the use of a base metal near to the pure metal [7, 8]. This can be rationalized by considering that the alloying element inducing a preferential grain-boundary diffusion is absent in the base metal. The present investigation examines the microstructure of the molten copper/solid iron interface and the appearance of molten copper upon migration into solid iron, because of the possible relevance of any interaction with the molten copper. The paper focuses on the migration kinetics and the interfacial microstructure formed in liquid/solid reaction couples at temperature ranging from 1100 to 1400° C.

2. Experimental methods

The solid metal used in this study was produced from commercial electrolytic iron (99.9 wt %). The iron was vacuum-melted in a high-alumina crucible at 1650° C, deoxidized and degassed by addition of a prepared Fe–4.4 wt % C alloy, and then cast into a metal mould 40 mm diameter. The castings (C = 0.06 wt %) were cut into specimen cylinders 30 mm diameter and 20 mm high. In the centre of the upper surface of the cylinder a hole was drilled 8 mm diameter and 4 mm deep. The interior of the hole, to be in contact with the molten metal, was polished with no. 1200 emery paper and degreased with reagent benzene.

Liquid metal samples were produced from electrolytic copper (99.9 wt %) and commercial silver (99.98 wt %). The copper was vacuum-melted in a high-alumina crucible at 1300° C and deoxidized by the introduction of hydrogen to prevent the formation of oxide film on the melt surface. The deoxidized copper (O_2 = 0.0003 wt %) was used as pure copper. In preparing Cu–Ag alloy samples, the electrolytic copper was melted under 0.027 MPa hydrogen when silver was added to the molten copper. The Cu–Ag alloys employed as the liquid metal sample were pure copper, Cu–4.65 wt % Ag, Cu–6.01 wt % Cu, Cu–6.76 wt % Ag and Cu–8.26 wt % Ag.

The experimental approach to the study of the interaction of molten metal with solid iron involved the use of plug tests as shown in Fig. 1. The copper sample, weighing approximately 1 to 2 g, was melted in the hole of the solid iron cylindrical specimen using a high-frequency induction furnace, i.e. the iron

0022–2461/86 $03.00 + .12

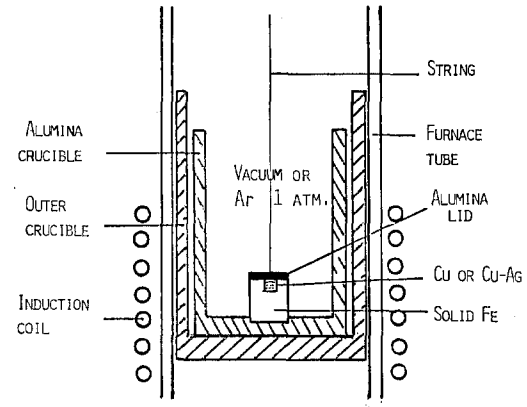

Figure 1 Reaction test by the melting of copper or Cu–Ag alloy in iron cylinder.

cylinder plugged with a lump of pure copper was rapidly heated under a vacuum of ~0.13 to 0.013 Pa for a selected time at a fixed temperature. Attainment of the fixed temperature requires 3 to 4 min. The temperature on the solid iron cylinder surface was measured using an optical pyrometer. The measured temperatures were 1100, 1150, 1200, 1300 and 1400° C, which were maintained to within ± 5° C of the desired temperature. The reaction time was 0 to 80 min. After the reaction was carried out, the specimen was cooled into the furnace under flowing argon gas. In the case of the Cu–Ag alloy plug, the surface of the iron cylinder was covered with an alumina lid and heated under 0.1 MPa argon, as shown in Fig. 1. This manipulation was necessary in order to prevent silver from vaporizing during the reaction. In this case, temperature measurements were obtained by opening the lid. The measured temperatures were 1200 and 1300° C and the reaction times ranges from 0 to 60 min.

After reaction the specimens were cross-sectioned, ground, and polished, etched with 5% nital and then examined metallographically. The solidified microstructure and the liquid metal migration appearance across the interface were observed using an optical microscope, and the migration depth was measured with a calibrated reticle at a magnification of × 400. Optical metallography was used because in the Cu–Fe metal system the Cu/Fe interface had a distinct and sharp dividing plane due to the extremely low mutual solubility of these two metals at room temperature. It was particularly convenient to use optical metallography for measurement of the migration depth.

3. Results and discussion

3.1. Mode of migration of molten metal into the solid metal

As soon as the molten metal makes contact with the solid metal, the migration of the molten metal into the solid metal and the dissolution of the solid metal in the molten metal takes place simultaneously.

It is thought that there are three basic reactions which occur at the liquid/solid interface upon migration, with the formation of a solid solution.

1. Incipient volume diffusion or lattice diffusion. Molten metal diffuses directly from the liquid–solid contact region into the base metal grain along the entire interfacial region. Accordingly, this diffusion causes the formation of a foreign atom-penetrated solid solution zone at the base metal surface.

2. Grain-boundary diffusion or short-circuit path. Liquid metal diffuses into the base metal along the grain boundaries. Then, after grain-boundary diffusion has occurred, the atoms migrate from the grain boundary into the lattice of the base metal (irrigation effects).

3. Grain-boundary penetration. The molten metal diffuses into the grain boundaries of the base metal. This grain-boundary diffusion and the alloying reaction occurring at the liquid/solid interface lower the interfacial surface-free energy, which promotes the grain-boundary wetting, resulting in deep penetration of molten metal into the grain boundary of the base metal.

In addition to the above migration mechanism, the dissolution and crystallization of solid metal at the liquid/solid metal interface can occur during dissimilar metal reaction [9]. This action means essentially that the dissolution of solid metal by molten metal and the subsequent dissolved metal deposition occur at constant atmospheric temperature through the process of crystallization and precipitation under certain conditions, and both are repeated. The crystallization and the growth of the solute in the molten metal seem to predominate at lower temperatures.

3.2. Microstructure of the liquid/solid interface

3.2.1. Microstructure of the Cu/Fe interface

The optical micrographs in Fig. 2 show the microstructures of the Cu/Fe interface at 1200 and 1300° C. The interaction of molten copper, i.e. the dissolution of solid iron into molten copper and the penetration of molten copper into solid iron, occur increasingly with increasing temperature and time. As a result, the increased interaction gives a greater amount of iron dendrite precipitated within the copper during solidification, and thicker reaction layers at the Cu/Fe interface. According to the Fe–Cu diagram [10] shown in Fig. 3, at this experimental temperature the solubility of copper in solid γ-iron is ~ 8 wt % and that of iron in molten copper is ~ 5 to 20 wt %. However, since the mutual solubility of these two metals is very low at room temperature, the liquid/solid interface will not disappear and will remain as a sharp dividing plane between the two metals. The enlarged microstructures of the Cu/Fe interface are shown in Fig. 4. Iron dendrites are crystallized within the copper (Figs. 4a and b). On the other hand, an iron dendrite layer growing towards the copper side and a copper solute layer penetrating into the iron surface are contiguous with each other at the Cu/Fe interface (Figs. 4c and d).

The Cu/Fe interfacial microstructure obtained by microscopic examination of the etched specimen is schematically shown in Fig. 5. The following six basic areas are shown [8, 11].

1. Iron dendrites in the copper matrix.
2. Eutectic/eutectoid copper matrix.

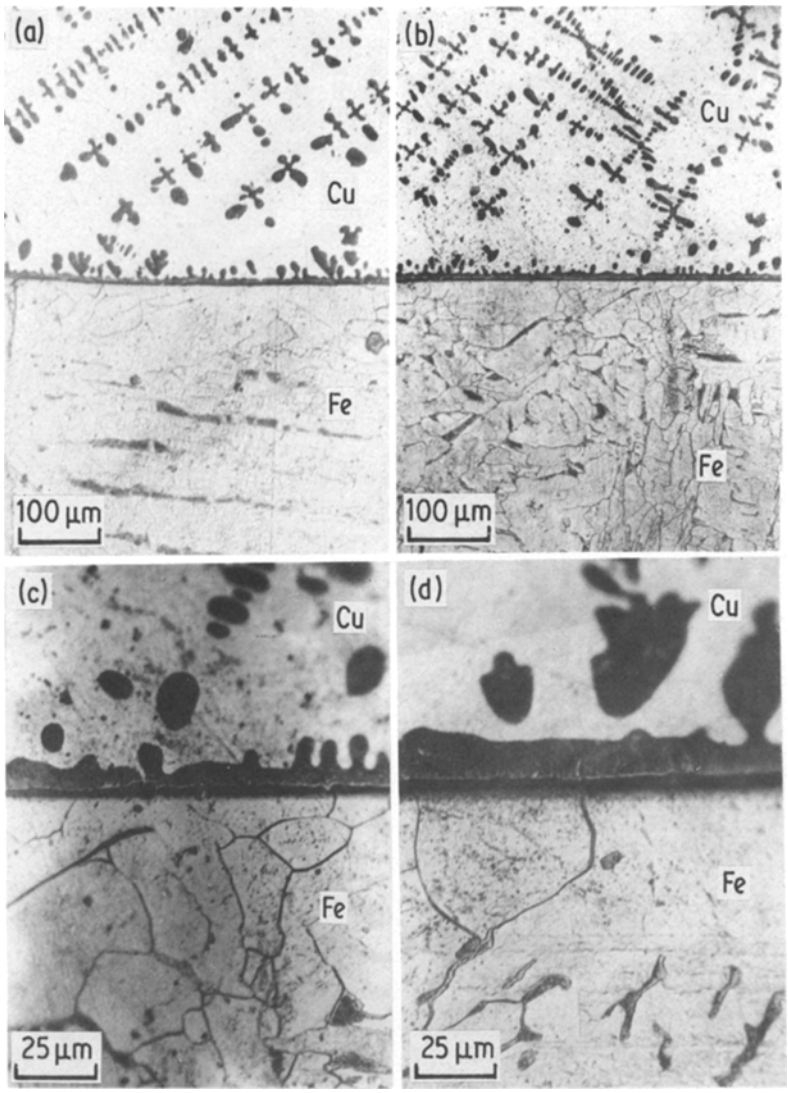

Figure 2 Optical micrographs of the Cu/Fe interface held at: (a) 1200° C (5 min), (b) 1300° C (0 min), (c) 1300° C (0 min), (d) 1300° C (3 min).

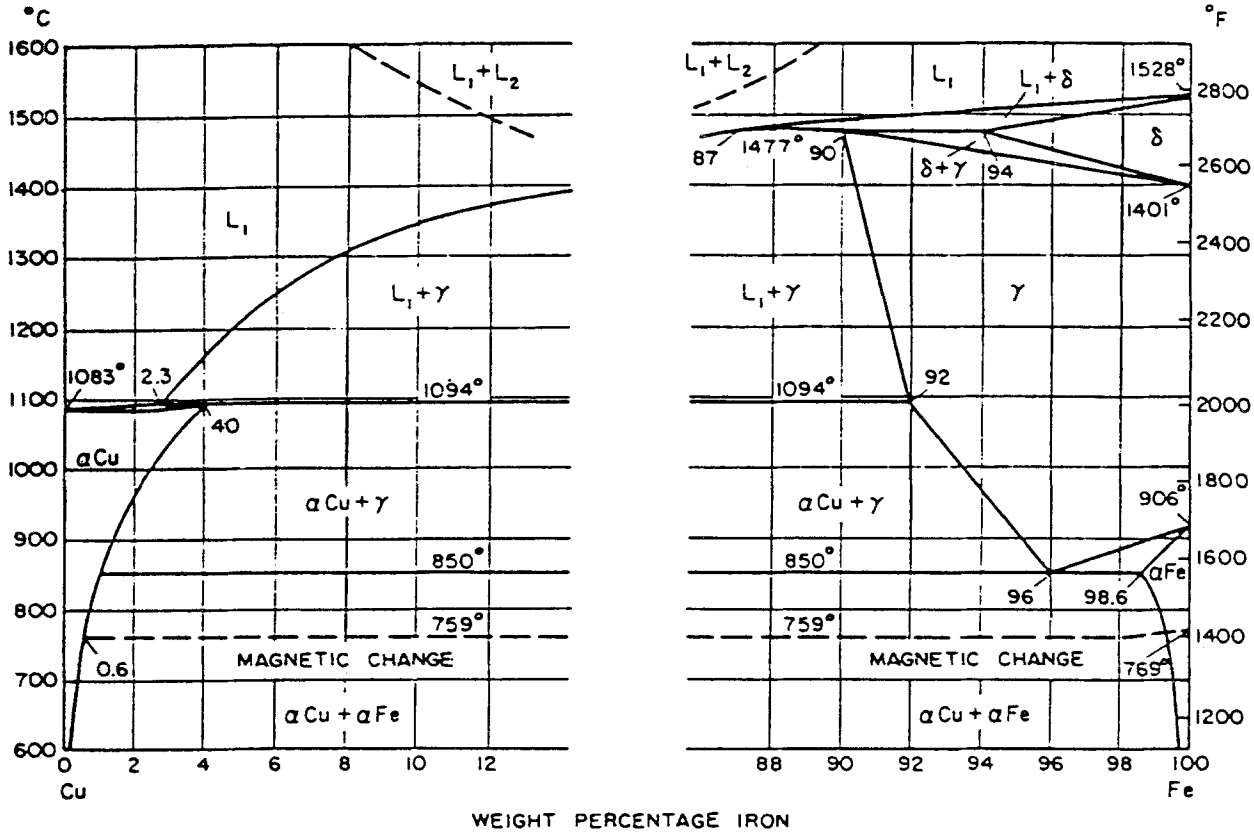

Figure 3 Diagram of the copper–iron system [10], indicating that in the liquid state also two phases L_1 and L_2 coexist with a partial solubility.

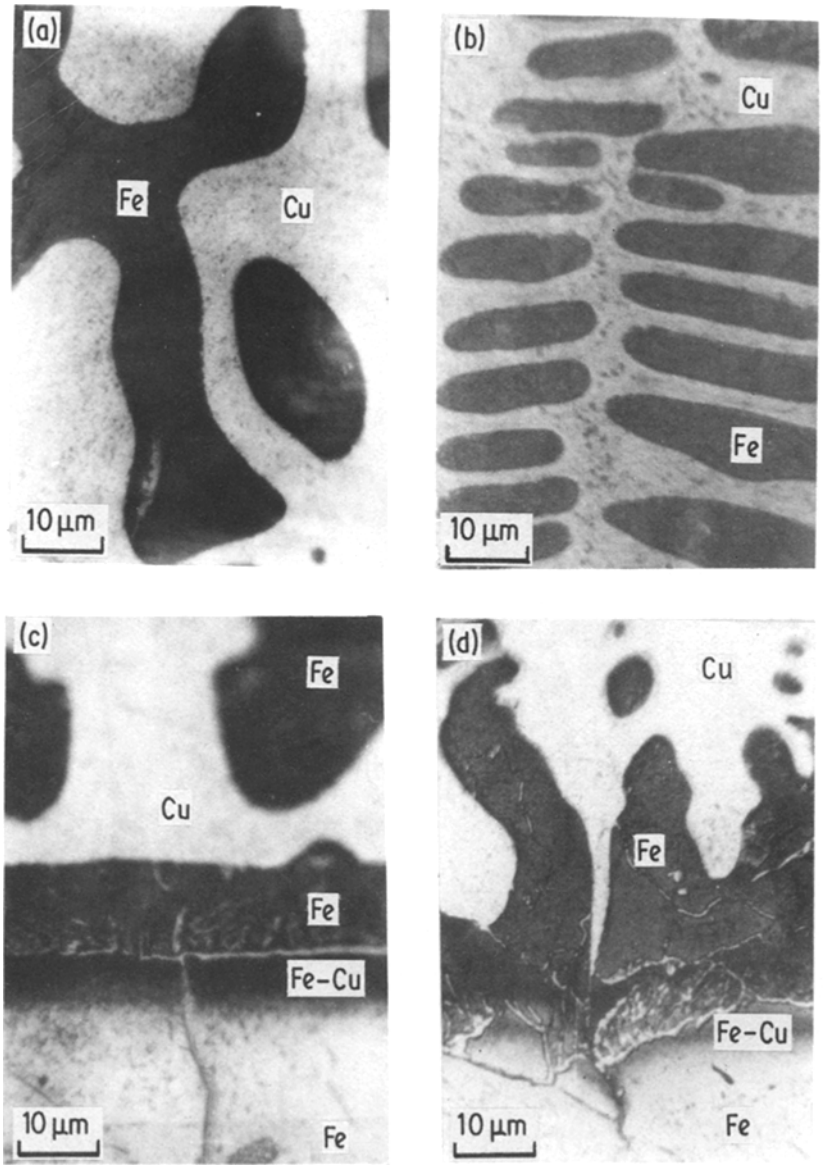

Figure 4 Enlarged micrographs of iron dendrites and the Cu/Fe interface. (a) Iron dendrites in the copper matrix treated at 1200° C for 5 min. (b) Many iron dendrites in the copper matrix treated at 1200° C for 15 min. (c) Regular Cu/Fe interface treated at 1300° C for 3 min. (d) Irregular Cu/Fe interface treated at 1300° C for 3 min.

3. Iron dendrite layer at the interface.
4. Copper-penetrated solid solution zone and decarburization.
5. Grain-boundary precipitates.
6. Unaffected solid iron.

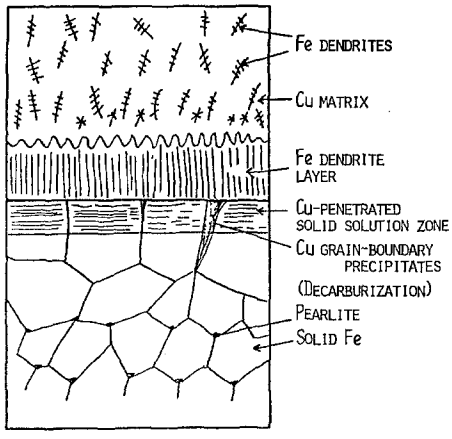

Figure 5 Schematic representation of the discrete regions in the heterogeneous boundary of the copper/iron interface.

Fig. 6 shows an example of the induced irrigation effect and grain-boundary penetration. At low temperatures, ranging from 1100 to 1200° C, the irrigation effect and grain-boundary penetration are likely to occur partially, while at high temperatures, ranging from 1300 to 1400° C, these phenomena are not observed, but a solid solution diffusion zone is recognized.

3.2.2. Microstructure of the Cu–Ag/Fe interface

Fig. 7 shows the microstructures of the Cu–6.01 wt % Ag/Fe interface. The structure of the Cu–Ag/Fe interface rarely changes metallographically as compared to that of the Cu/Fe interface. However, the inactivation of the reaction between copper and iron, caused by the addition of silver to the molten copper makes the amount of iron dendrite crystallized within the copper decrease, and the reaction layers at the interface (such as the dendrite layer and solid solution zone) to become thinner. The rounded shape of these precipitated dendrites can easily be recognized in Fig. 7, in comparison with the slightly radial shape at the Cu/Fe interface. Furthermore, grain-boundary

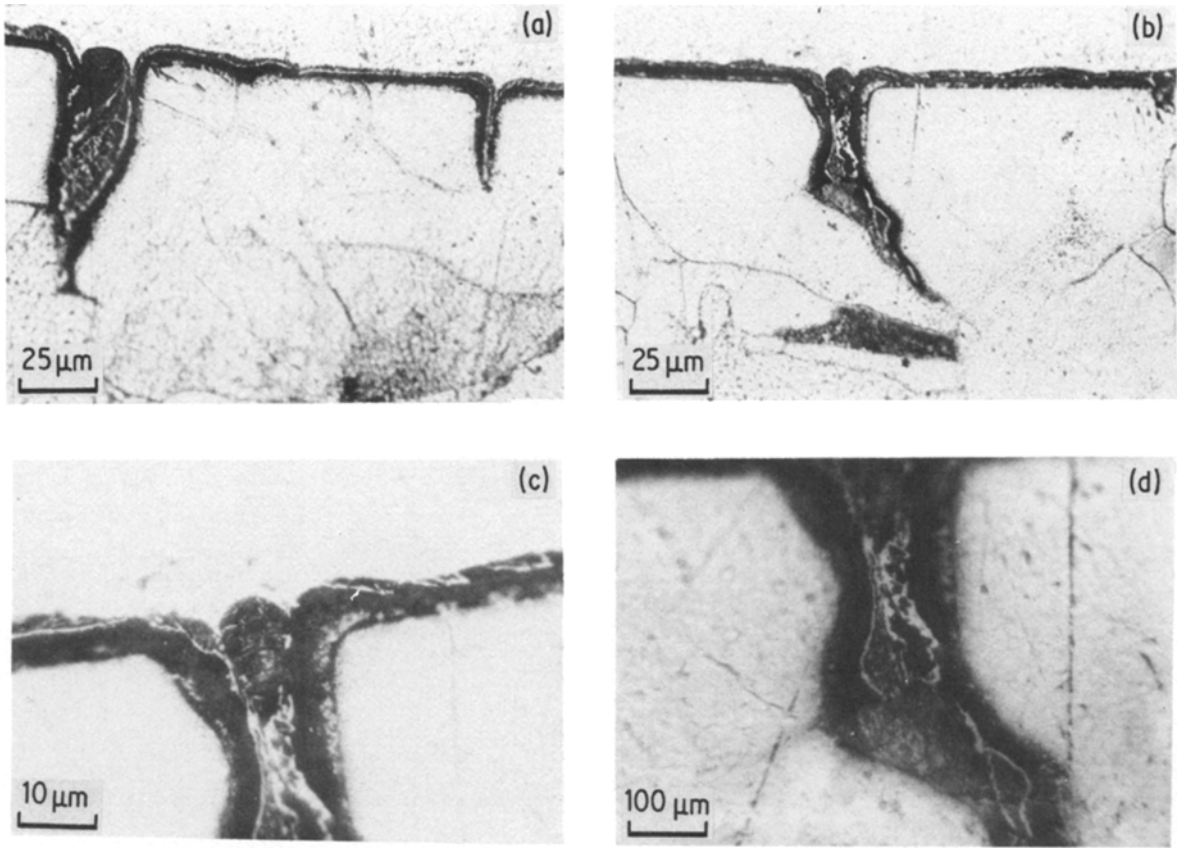

Figure 6 Optical micrographs of irrigation effects and grain-boundary penetration at 1200° C for 50 min. (a), (b) Micrographs showing an example of grain boundary diffusion, irrigation effect and grain-boundary penetration. (c), (d) Enlarged micrographs of copper precipitates at the grain boundary and solid solution layer produced by irrigation effects at the grains in the neighbourhood of the grain boundary.

diffusion, irrigation effect and grain-boundary penetration are unlikely to occur.

3.3. The migration kinetics of molten copper into solid iron

The actual situation for the migration of molten copper into the solid iron, i.e. the evolution of the reaction between molten copper and solid iron, is shown schematically in Fig. 8. The migration of molten copper into the solid iron is initiated by the dissolution of solid iron in the molten copper as a result of contact between copper and solid iron (Fig. 8a). An iron-saturated layer on the molten copper side of the Cu/Fe interface and a copper-penetrated solid solution zone on the solid iron surface, begin to form thinly (Fig. 8b). Furthermore, the presence of a large amount of iron solute in the molten copper, due to iron dissolution, causes the liquid concentration to approach the saturated concentration with elapse of time, as it has been shown that large evolution of the iron-saturated layer and the solid solution zone at the interface, and both grain-boundary diffusion and decarburization in the iron surface, occur simultaneously (Fig. 8c). This decarburization is caused by the carbon in the base metal diffusing into the iron surface layer, where the copper is penetrating. Therefore, it is thought that the diffusion of carbon into the solid iron surface results in the formation of an Fe–Cu–C layer at the iron surface.

From these direct observations, the thickness of the copper-penetrated layer zone, formed by the migration of molten copper into solid iron along the entire interfacial region, was measured. This layer formation is due to direct solid solution diffusion. The average thickness of this layer, W, after a selected time, t, at each of the selected temperatures, was plotted in Fig. 9. The penetrated depth increases parabolically with reaction time. The penetration rate, dW/dt may be inversely proportional to the penetrated layer thickness, W [12], that is,

$$\frac{dW}{dt} = K_w \frac{1}{W} \quad (1)$$

where K_w is the penetration rate constant ($cm^2 sec^{-1}$) at the selected temperature. Upon integration, this gives:

$$W^2 - W_0^2 = 2K_w t \quad (2)$$

where W_0 is the penetrated thickness at time $t = 0$. Fig. 10 shows the plot of $W^2 - W_0^2$ against t for the different temperatures. The proportionality indicates that the penetration of molten copper into solid iron is controlled by diffusion. The values of the penetration rate constant are derived from the slopes in Fig. 10. The activation energy characterizing the penetration of the layer was determined on the usual assumption that the dependence of K_w on temperature is expressed as

$$K_w = K_0 \exp\left(-\frac{Q}{RT}\right) \quad (3)$$

where K_0 is a constant, Q is the activation energy and

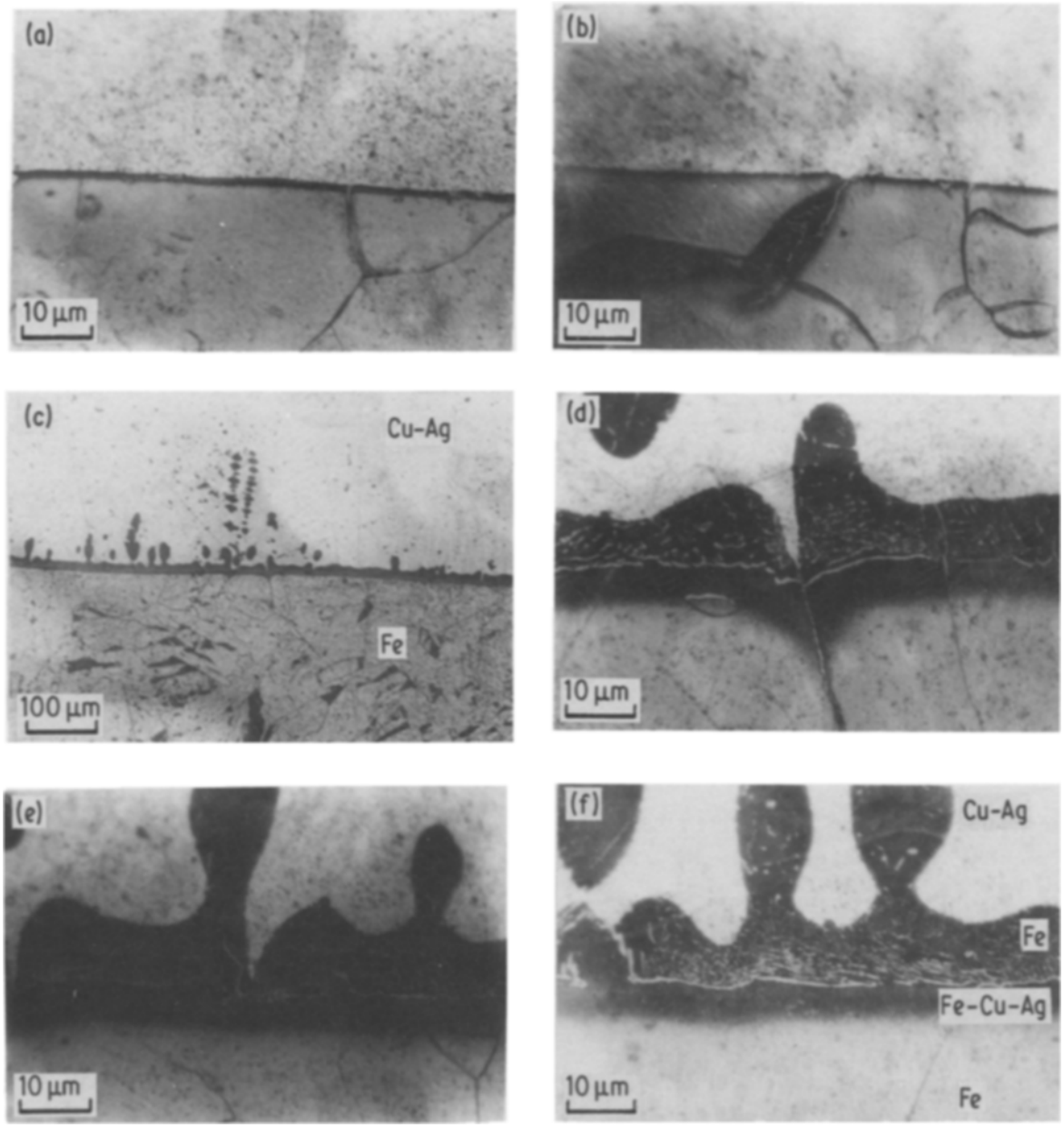

Figure 7 Optical micrographs of the Cu–6.01 wt % Ag/Fe interface. (a), (b) Enlarged micrographs of the Cu–Ag/Fe interface (1100° C, 80 min). (c) Cu–Ag/Fe interface structure (1200°C, 60 min). (d) to (f) Enlarged micrographs of the Cu–Ag/Fe interface having various shapes (1200° C, 60 min).

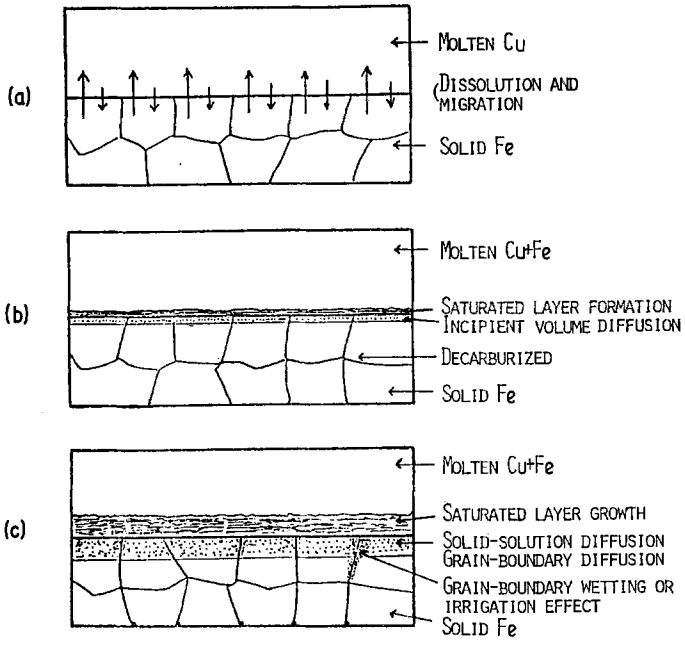

Figure 8 Development of the interface between molten copper and solid iron. (a) The migration of molten copper into iron occurs simultaneously with the gross dissolution of iron into molten copper. (b) The iron-saturated layer and copper-penetrated solid solution zone formed at the liquid/solid interface. (c) The iron-saturated layer and copper-penetrated zone evolving opposite each other, and the short-circuit path and irrigation effect partially occurring.

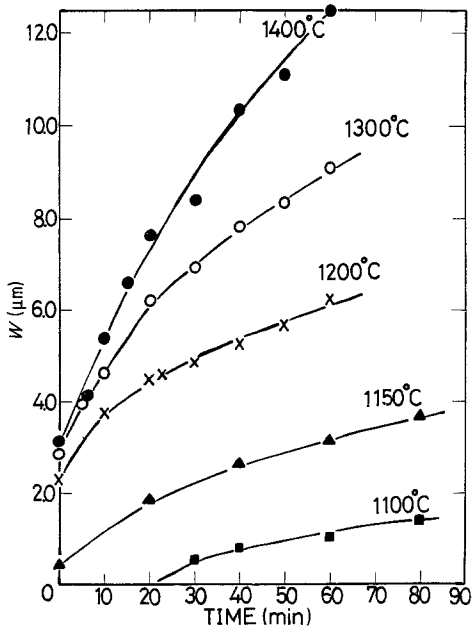

Figure 9 Migration of molten copper into solid iron at temperatures ranging from 1100 to 1400° C.

T is the absolute temperature. The result of this analysis is shown in Fig. 11 and is summarized in Table I. The activation energy value determined here is approximately close to the value of 255.2 kJ mol^{-1} measured by Linder and Karnik [13] for the diffusion of copper into iron in the temperature range 800 to 1200° C, that of 306.7 kJ mol^{-1} given by Rothman *et al.* [14] at temperatures ranging from 1285 to 1368° C, and that of 305.0 kJ mol^{-1} reported by Majima and Mitani [15] at temperatures ranging from 1105 to 1210° C. It is obvious that the estimation of these reference values is valid in comparison with the activation energy obtained in this experiment.

Fig. 12 indicates the relationship between penetration depth and heating temperature for the migration of molten copper into solid iron. A bend in

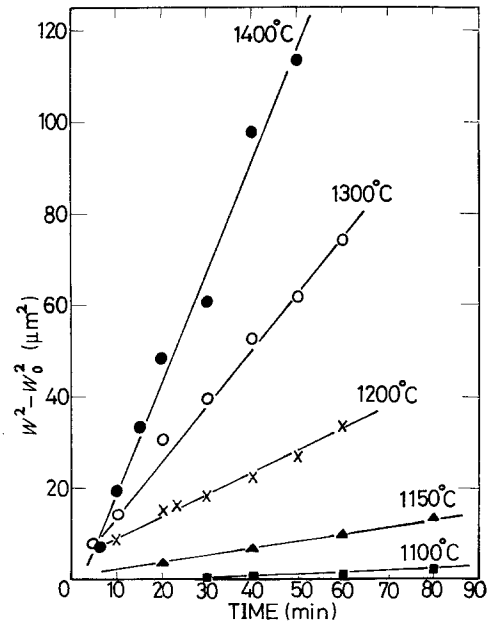

Figure 10 The plots of $W^2 - W_0^2$ against t for the migration of molten copper into solid iron.

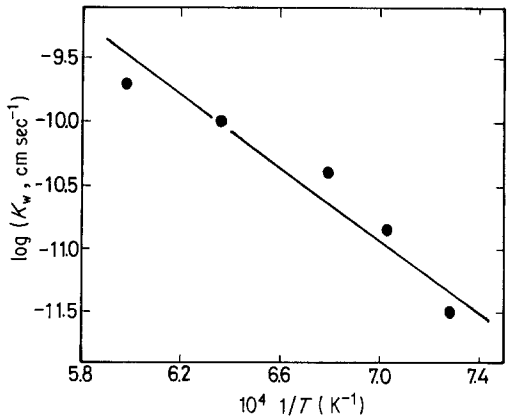

Figure 11 The temperature dependence of the penetration rate constant for the migration of molten copper into solid iron.

the curve is observed in the neighbourhood of 1200° C. This may be due to the progress of migration with a mechanism different from that in the low and the high temperature regions. Rothman *et al.* [14] found that in the diffusion of copper in iron at temperatures higher than 1285° C, the volume diffusion predominated in the γ-phase. The work of Rolls and Badelek [16] has shown that with mild steel (0.2 wt % C), both grain-boundary and volume diffusion can be encountered at temperatures between 1100 and 1200° C. In our experiment, also, it is observed that the characteristic modes of penetration of copper into iron are predominantly by volume diffusion at temperatures above 1200° C and by both volume and intergranular diffusion at lower temperatures as can be seen in Figs. 2 and 6. From these results, it may be surmised that the migration is dominated largely by volume diffusion at temperatures exceeding ~ 1200° C and by both volume and grain-boundary diffusion at lower temperatures.

3.4. Effect of silver on the migration of molten Cu–Ag alloy into solid iron

Experiments to study the effect of silver on migration were carried out at 1200 and 1300° C for selected time intervals with silver concentrations of 4.65, 6.76 and 8.26 wt %. Figs. 13 and 14 show the plots of the penetration depth of molten Cu–Ag into iron against

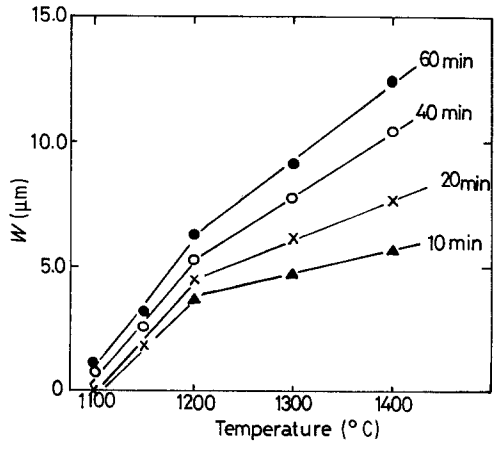

Figure 12 Relationship between penetration depth and heating temperature for the migration of molten copper into solid iron.

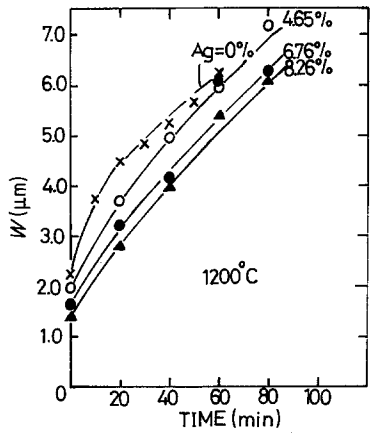

Figure 13 Effect of silver on the penetration depth of molten Cu–Ag alloy into solid iron at 1200° C.

reaction time for different silver concentrations and temperatures. The copper-penetrated layer thickness decreases with increasing silver concentration. At 1200° C the penetration rate varies little with increase in reaction time, but at 1300° C the rate is especially lowered with the time, the degree of lowering being higher for high silver concentrations. In plotting $W^2-W_0^2$ against t for the migration of molten Cu–Ag into solid iron, a linear relationship is observed, as shown in Figs. 15 and 16 at temperatures of 1200 and 1300° C, respectively. From the slope of the straight line the penetration rate constant, K_w can be obtained and the data are presented in Table I. Fig. 17 shows the effect of addition of silver to the molten copper on the rate constant, indicating that the rate constant decreases with an increased silver concentration, in which the decrease is more pronounced at 1300° C.

4. Conclusions

The interaction of solid iron with molten copper has been investigated in order to elucidate the microstructures of the Cu/Fe and Cu–Ag/Fe interface and the migration mechanism of molten copper and Cu–Ag alloy into solid iron. The principal results obtained from this analysis are summarized below.

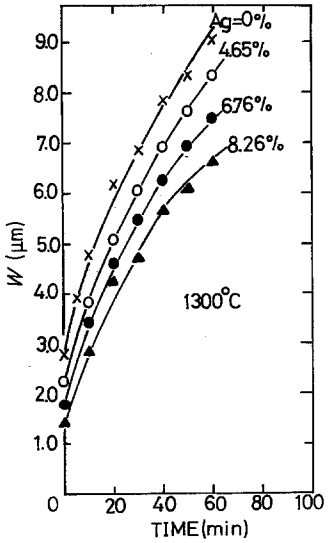

Figure 14 Effect of silver on the penetration depth of molten Cu–Ag alloy into solid iron at 1300° C.

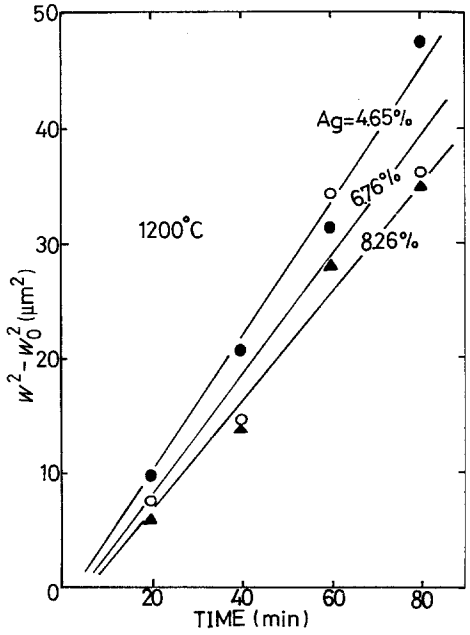

Figure 15 The plots of $W^2 - W_0^2$ against t for the migration of molten Cu–Ag alloy into solid iron at 1200° C.

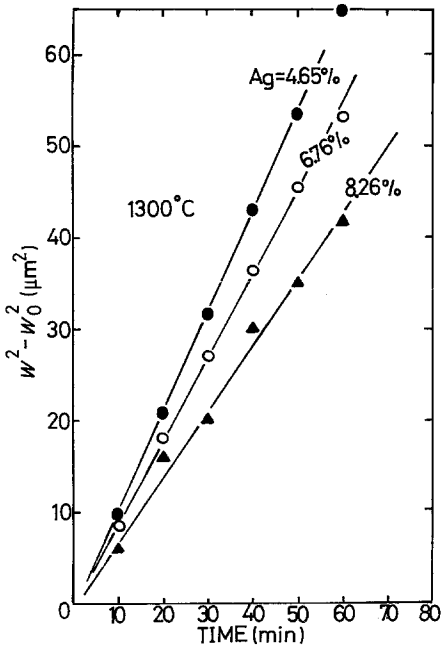

Figure 16 The plots of $W^2 - W_0^2$ against t for the migration of molten Cu–Ag alloy into solid iron at 1300° C.

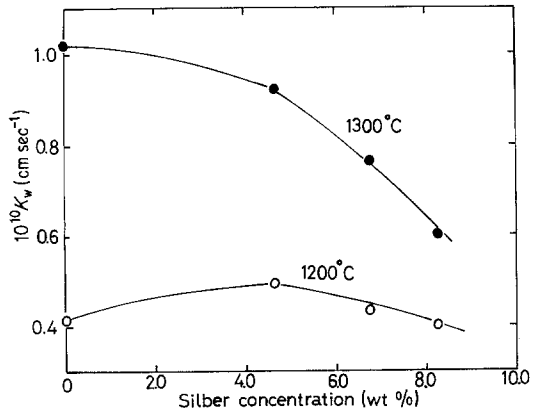

Figure 17 Relationship between penetration rate constant and silver concentration.

TABLE I Data on the migration of molten copper and Cu–Ag alloy into solid iron

Temperature (°C)	Migration of molten copper into solid iron		Migration of molten Cu–Ag alloy into solid iron, $K_w(10^{-10}\,cm\,sec^{-1})$		
	$K_w(10^{-10}\,cm\,sec^{-1})$	$Q(kJ\,mol^{-1})$	4.65 wt % Ag	6.76 wt % Ag	8.26 wt % Ag
1100	0.0313	277.8	–	–	–
1150	0.143	277.8	–	–	–
1200	0.414	277.8	0.496	0.434	0.404
1300	1.02	277.8	0.922	0.763	0.602
1400	2.01	277.8	–	–	–

1. The microstructure of the Cu/Fe interface consists of iron dendrites in the copper matrix, an iron dendrite layer and a copper-penetrated zone at the interface, and grain-boundary precipitates and decarburization in part in the solid iron surface. At low temperatures, an irrigation effect and grain-boundary penetration were observed partially.

2. The inactivation of the reaction caused by the addition of silver to the molten copper, reduces the thickness of the layer formed at the liquid/solid interface.

3. The migration of molten copper into iron occurs mainly by the formation and growth of an iron-saturated layer due to iron dissolution in molten copper and a copper-penetrated solid solution zone due to incipient volume diffusion.

4. The thickness of the copper-penetrated layer formed during the reaction follows parabolic kinetics and the penetration appears to be chiefly dominated by volume diffusion at high temperatures and by both volume and grain-boundary diffusion at low temperatures.

5. An increase of silver content in the molten copper retards the penetration rate constant.

Acknowledgements

I would like to thank Messrs S. Yamada and K. Enami for the performance of this experiment and Professor Y. Syono for the helpful advice on this work.

References

1. S. J. MATTHEWS and W. F. SAVAGE, *Weld. J.* **50** (1971) 174s.
2. R. J. SCHLAGER and D. L. OLSON, *J. Nucl. Mater.* **57** (1975) 312.
3. V. LAMPE, H. ROOS and M. SVENSSON, *Werk. u. Korro.* **28** (1977) 226.
4. I. AMATO, F. BAUDROCCO and M. RAVIZZA, *Weld. J.* **50** (1971) 183s.
5. N. BREDZS and H. SCHWARTZBART, *ibid.* **38** (1959) 305s.
6. W. F. SAVAGE, E. F. NIPPES and R. P. STANTON, *ibid.* **57** (1978) 9s.
7. T. ISHIDA, *Sci. Rep. Res. Inst. Tohoku Univ. A* **22** (1970) 18.
8. *Idem, Trans. Jpn Weld. Soc.* **3** (1972) 7.
9. T. YOSHIDA and H. OHMURA, *Weld. J.* **64** (1985) 1s.
10. A. BUTTS, "The Metal, Its Alloys and Compounds" (Reinhold, New York, 1954) p. 471.
11. S. LAMB and F. M. MILLER, *Weld. J.* **48** (1969) 283s.
12. W. JOST, "Diffusion in Solids, Liquids and Gases" (Academic, New York, 1952) p. 341.
13. R. LINDER and F. KARNIK, *Acta Metall.* **3** (1955) 297.
14. S. J. ROTHMAN, N. L. PETERSON, C. M. WALTER and L. J. NOWIAKI, *J. Appl. Phys.* **39** (1968) 5041.
15. K. MAJIMA and H. MITANI, *Trans. Jpn Inst. Metals* **19** (1978) 663.
16. R. ROLLS and P. S. C. BADELEK, *J. Iron Steel Inst.* **209** (1971) 149.

Received 22 March
and accepted 31 May 1985